Supplementary Information

pH-clock programmed autonomous bidirectional actuation and optical modulation of a multi-stimuli-responsive hydrogel

Sampurna Routray, Priyam Das, Malay Kumar Baroi, Debapratim Das*

Department of Chemistry, Indian Institute of Technology Guwahati, North Guwahati, Assam 781039, India. Email: ddas@iitg.ac.in

Supporting Figures

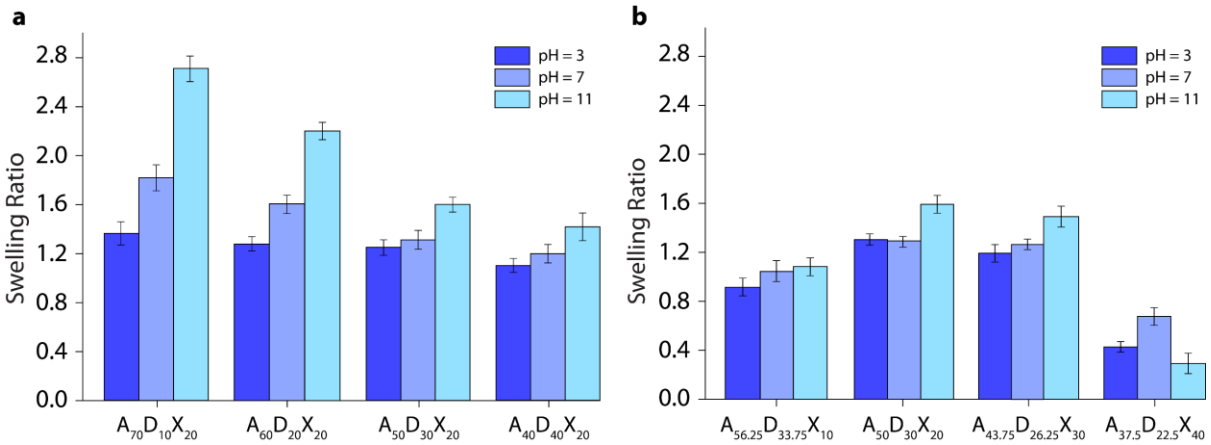

Figure S1. Swelling ratios of different combinations of the bilayered hydrogels at three different pHs. **a,** $A_mD_nX_{20}$, and **b,** $A_mD_nX_o$ (m:n = 5:3).

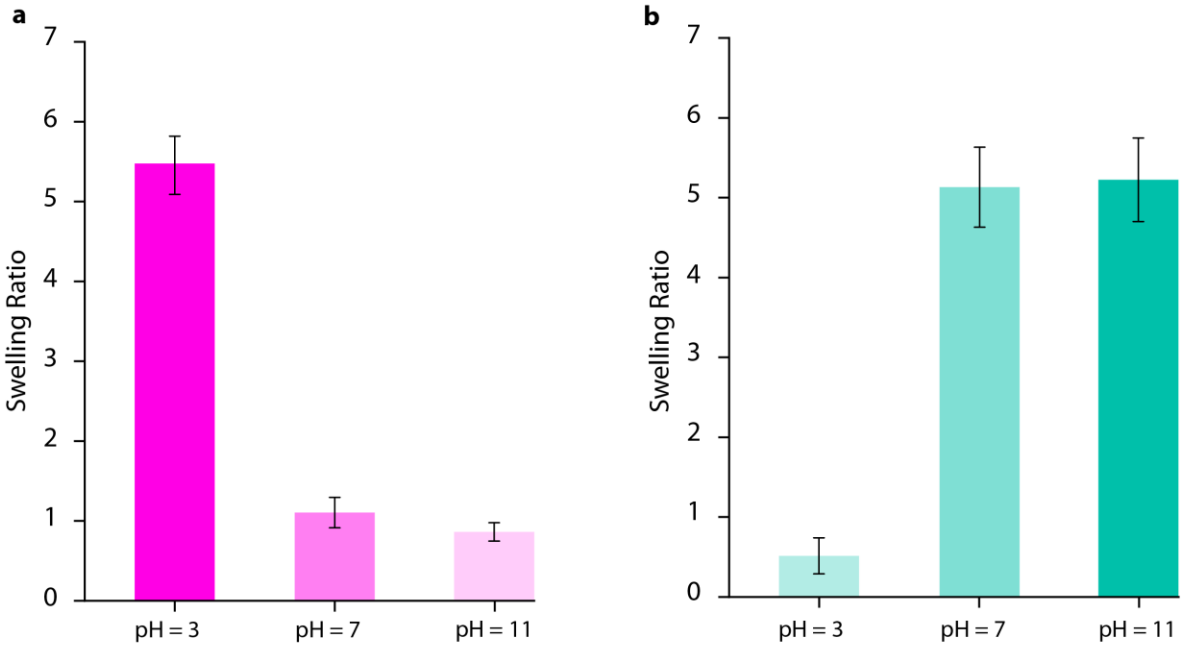

Figure S2. Swelling ratios of the **a,** VIm@AAm, and **b,** MAA@AAm layers of HA at three different pHs.

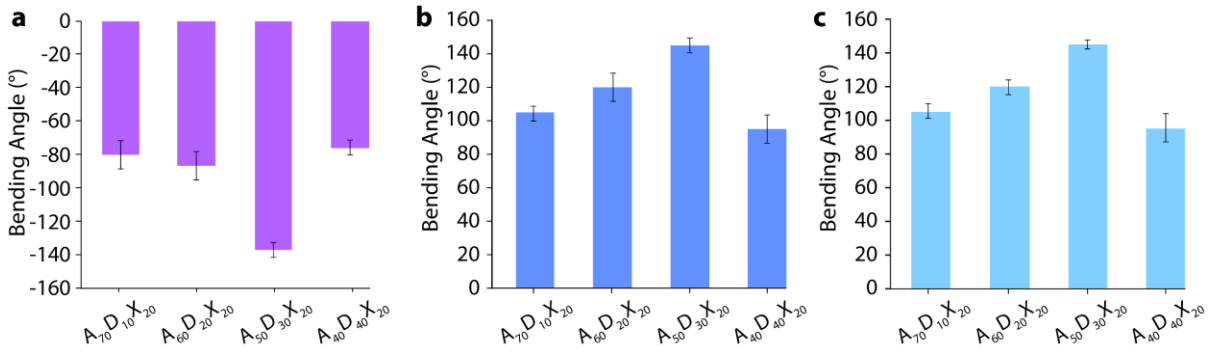

Figure S3. Bending angles of the combinations of the $A_mD_nX_{20}$ hydrogels at pHs. **a,** pH 3, **b,** pH 7, and **c,** pH 11.

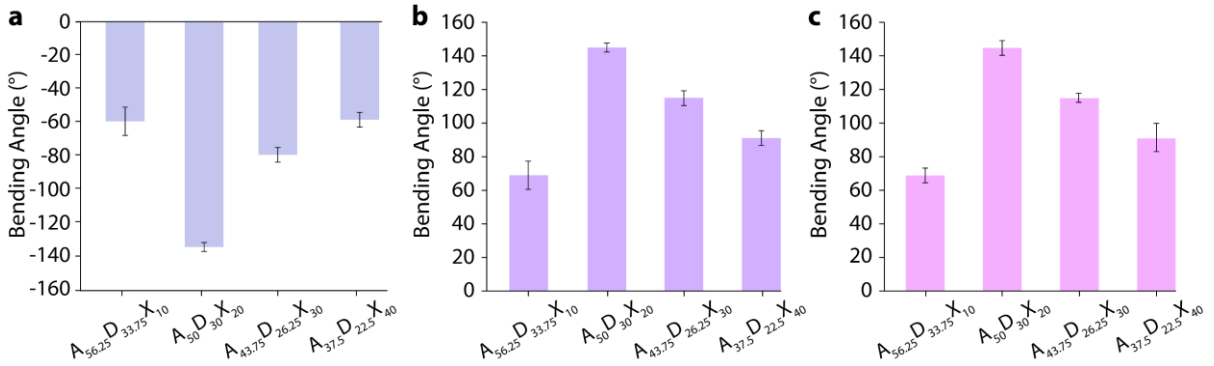

Figure S4. Bending angles of the combinations of the $A_mD_nX_o$ hydrogels; keeping the AAm – DMAA ratio fixed at 5:3, at pH **a,** 3, **b,** 7, and **c,** 11.

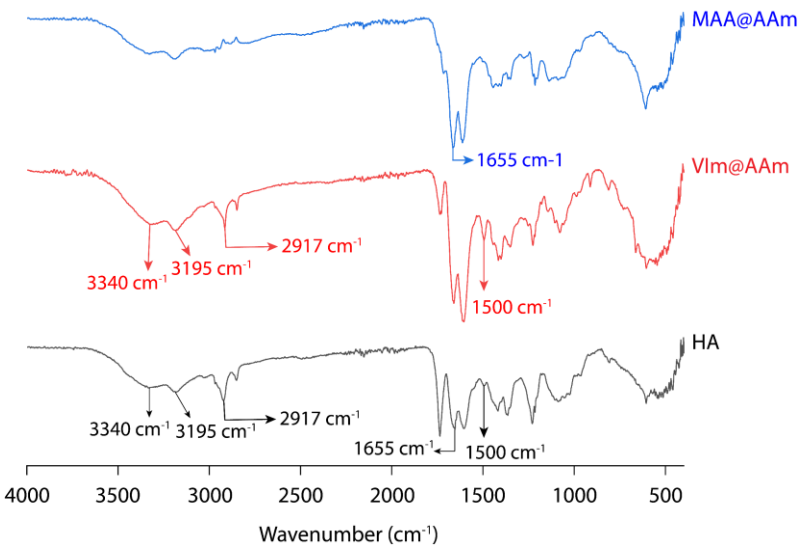

Figure S5. FTIR spectra of the individual layers and HA.

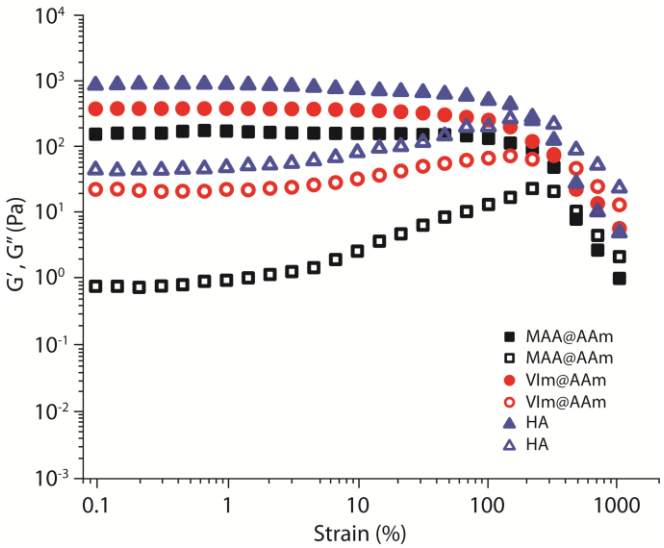

Figure S6. Rheological studies of the individual layers and HA.

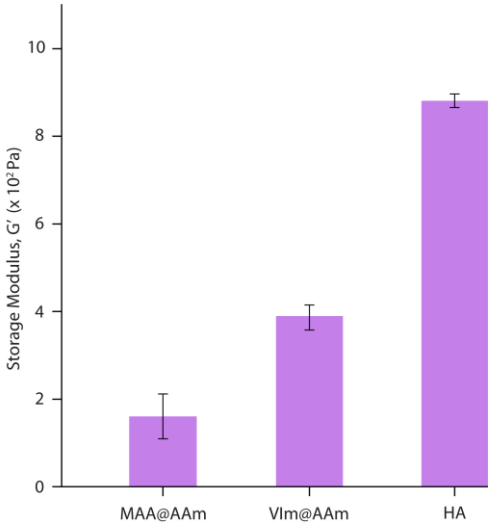

Figure S7. Comparison of the storage modulus of the individual layers and HA.

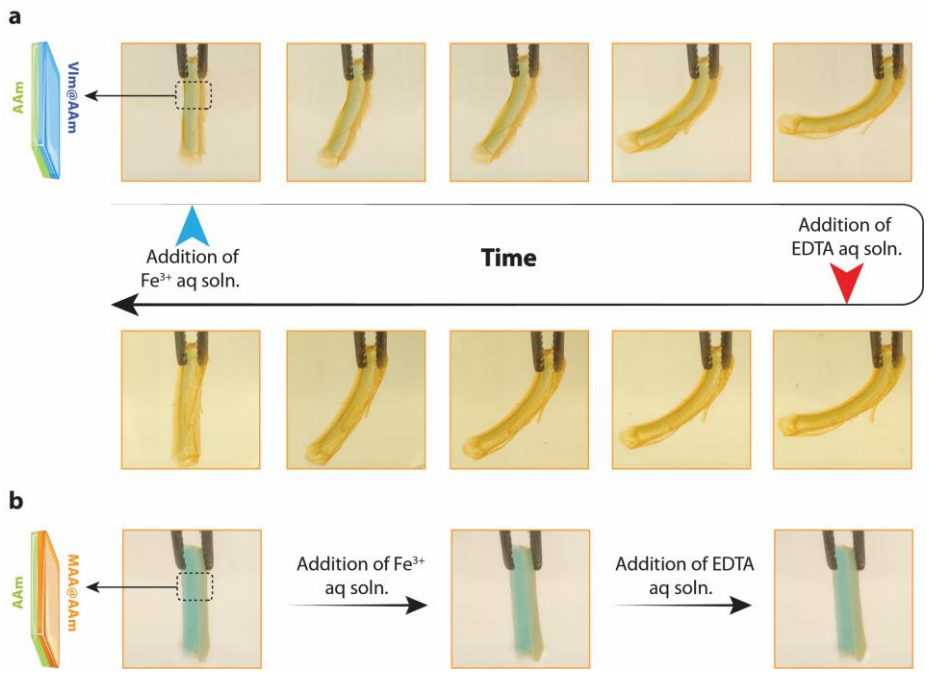

Figure S8. Actuation performances of the control bilayered hydrogels in the presence of Fe^{3+} (10 mM) and EDTA (25 mM). **a,** One layer of AAm and another with Vim@VIm. **b,** One layer of AAm and another with MAA@AAm.

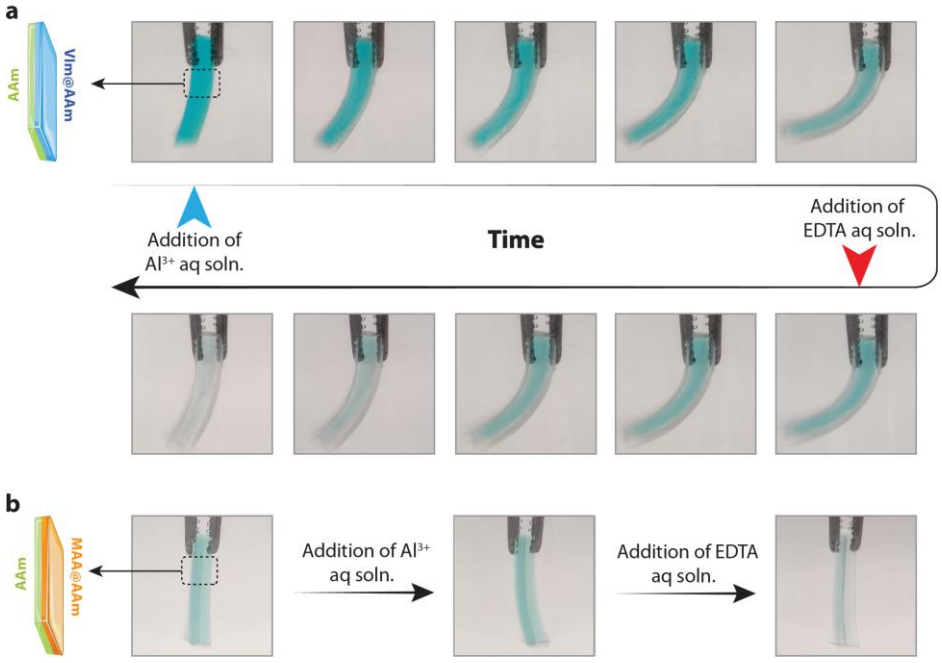

Figure S9. Actuation Performances of the control bilayered hydrogels in the presence of Al^{3+} (10 mM) and EDTA (25 mM). A) One layer of AAm and another with Vim@VIm. B) One layer of AAm and another with MAA@AAm.

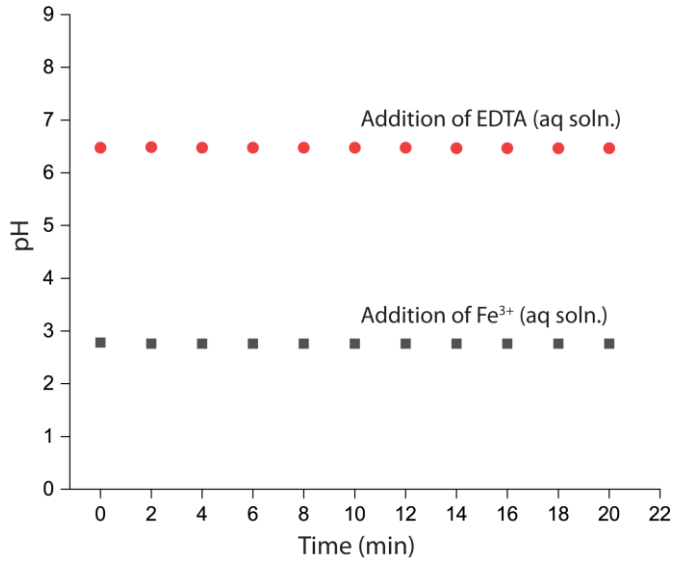

Figure S10. Change in the pH of the bulk aqueous solution in the presence of Fe^{3+} (10 mM) and EDTA (25 mM).

Control experiment for Fe^{3+}-responsive bending deformation: We performed two control experiments to assess the Fe^{3+}-responsiveness of HA. First, we studied the bending deformation of the actuator in the presence of Fe^{3+} aqueous solution (10 mM). Second, we investigated the same with an aqueous solution of similar acidic pH. $FeCl_3$ metal salt, upon being added to the bulk aqueous medium, reduces the pH of the system as a whole (~ 3.0). Therefore, we conducted the actuation experiment of the bilayered hydrogel in an aqueous solution of similar pH. The acidic solution was made with a very minimal concentration of HCl (1 mM). It was found that for Fe3+ ions, actuation was faster. Further, under acidic conditions, it took longer.

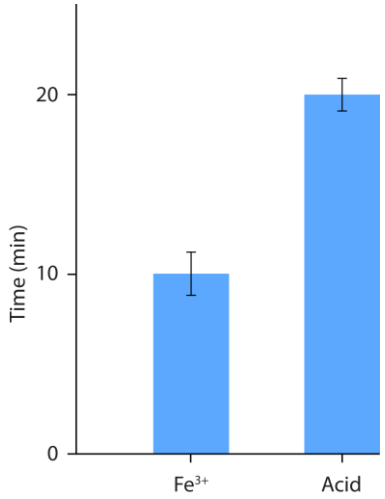

Figure S11. Time of bending deformation of HA in the presence of Fe^{3+} metal ions (10mM) and an acidic solution of pH 3.

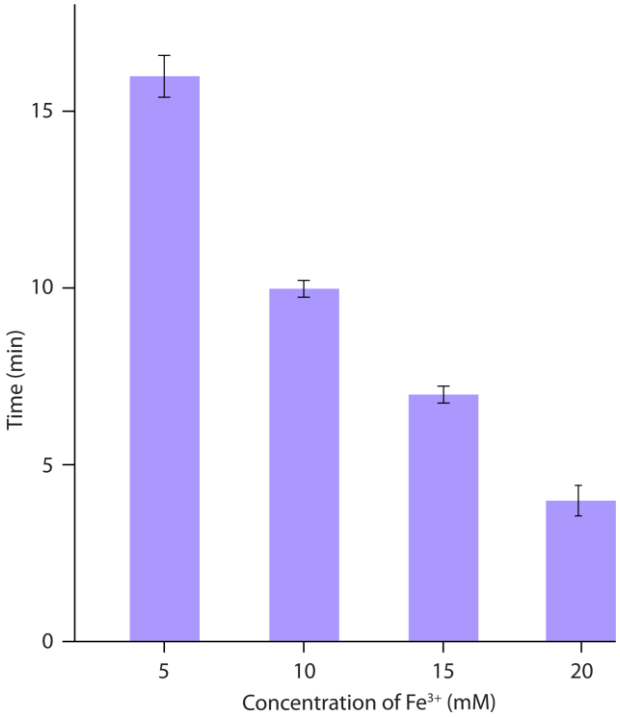

Figure S12. Time of bending deformation of HA in the presence of different concentrations of Fe^{3+} metal ions.

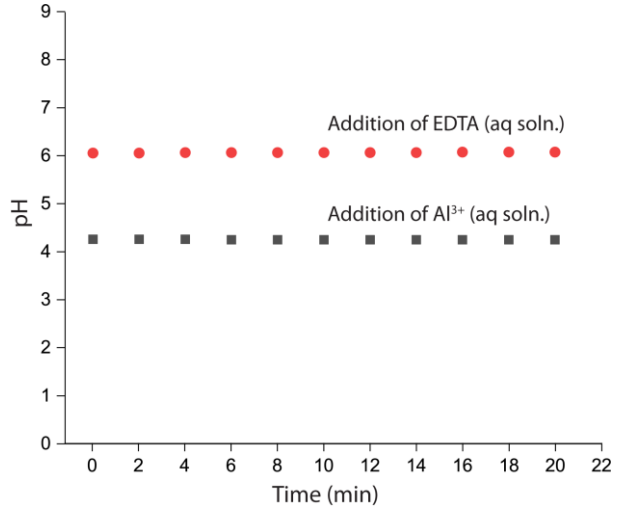

Figure S13. Change in the pH of the bulk aqueous solution in the presence of Al^{3+} (10 mM) and EDTA (25 mM).

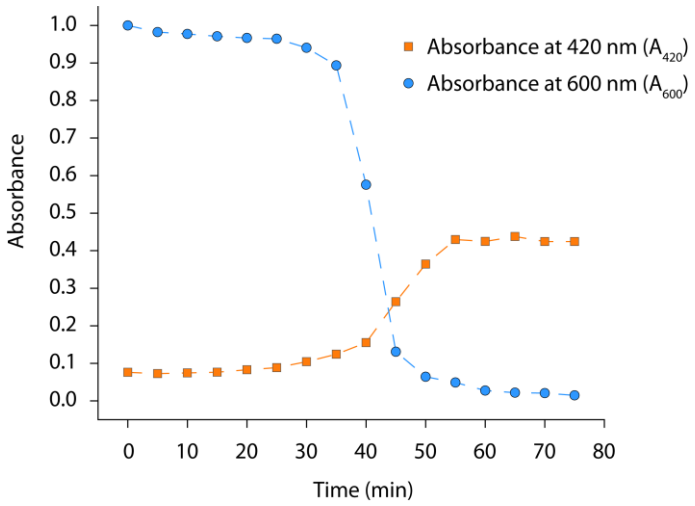

Figure S14. Time-dependent absorbance values of the TB dye with the dynamic pH variation of the NaOH-Sul (2:25 mM) clock.

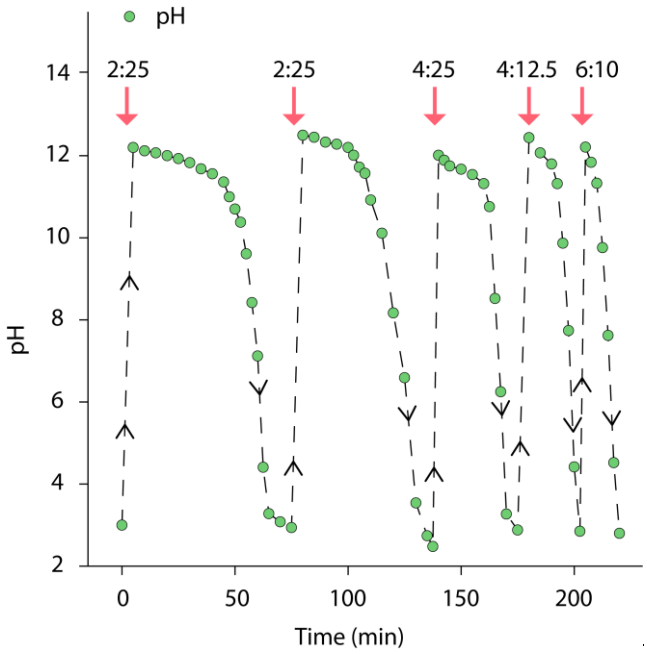

Figure S15. Adaptability of the NaOH-Sul pH-clock at various concentrations.

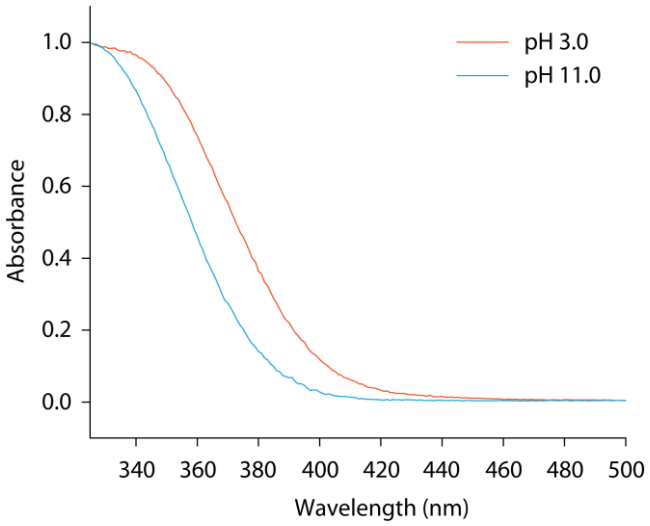

Figure S16. pH-dependent absorption spectra of TPE4A.

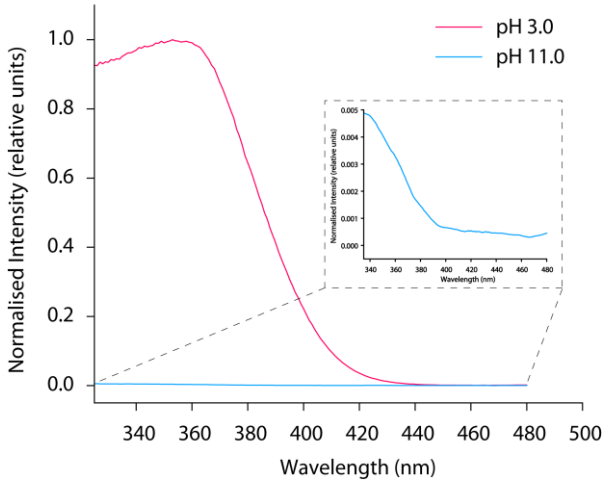

Figure S17. pH-dependent excitation spectra of TPE4A.

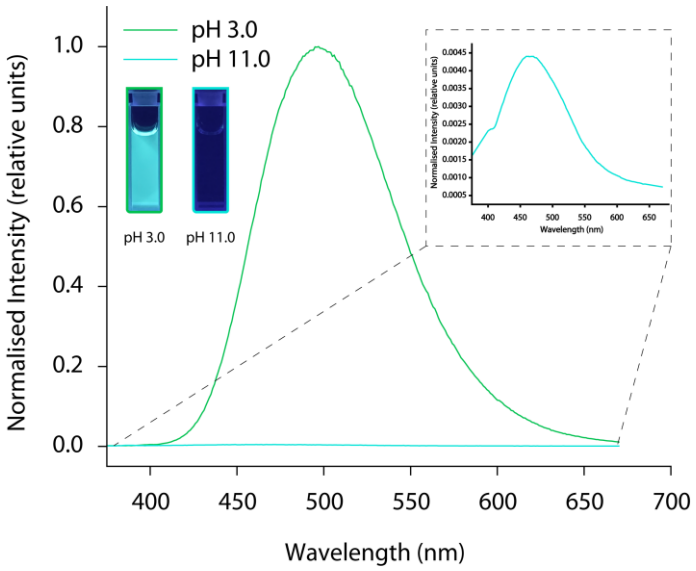

Figure S18. pH-dependent emission spectra of TPE4A.

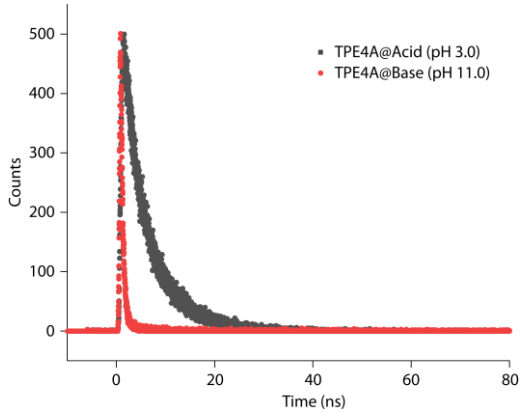

Figure S19. pH-dependent fluorescence decay profiles of TPE4A.

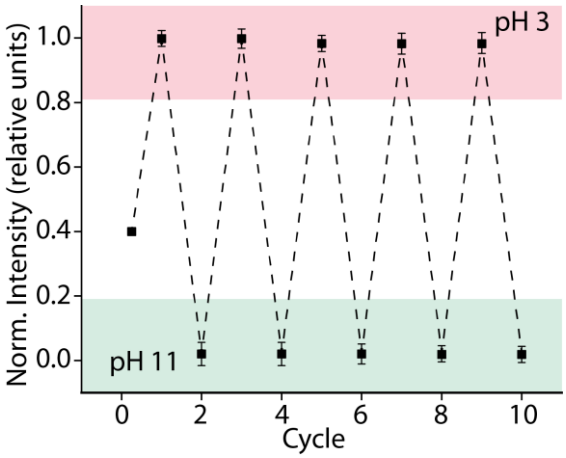

Figure S20. pH-dependent reversible cycles exhibited by TPE4A.

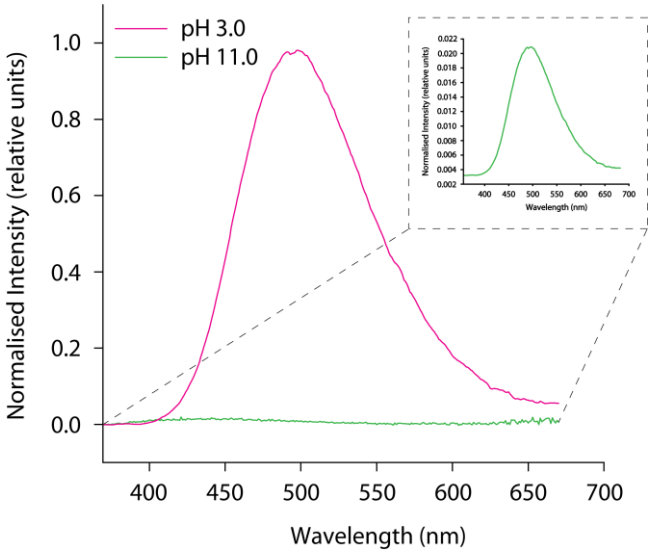

Figure S21. pH-dependent emission spectra of TPE4A@HA.

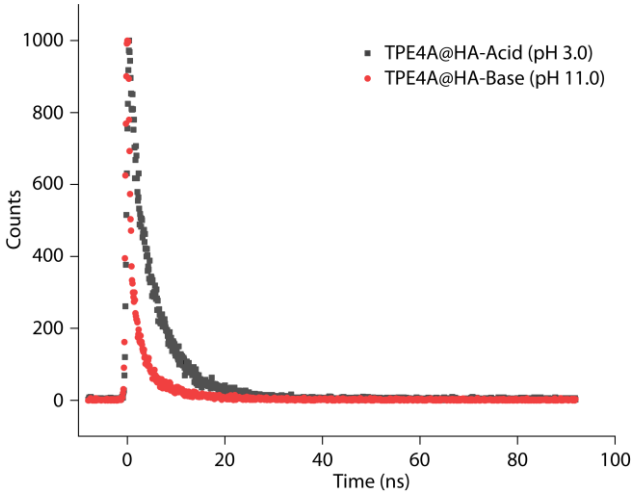

Figure S22. pH-dependent fluorescence decay profiles of TPE4A@HA.

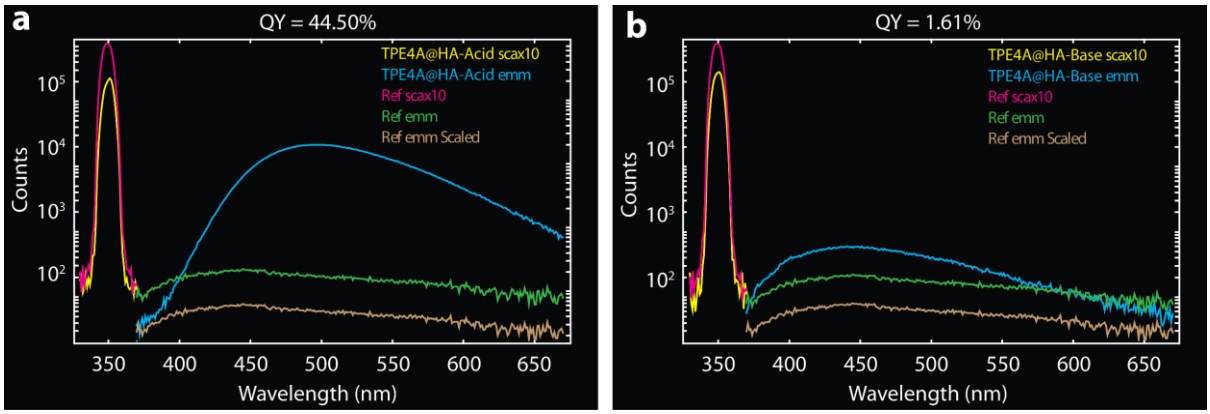

Figure S23. Quantum yields of TPE4A@HA at pH **a,** 3, and **b,** 11.

Table S1. Compositions of the various $A_mD_nX_{20}$ bilayered hydrogels.

Entry	Sample	Composition (wt%)						
1	$A_{70}D_{10}X_{20}$	**1st layer**	AAm	70	DMAA	10	VIm	20
		2nd layer	AAm	70	DMAA	10	MAA	20
2	$A_{60}D_{20}X_{20}$	**1st layer**	AAm	60	DMAA	20	VIm	20
		2nd layer	AAm	60	DMAA	20	MAA	20
3	$A_{50}D_{30}X_{20}$	**1st layer**	AAm	50	DMAA	30	VIm	20
		2nd layer	AAm	50	DMAA	30	MAA	20
4	$A_{40}D_{40}X_{20}$	**1st layer**	AAm	40	DMAA	40	VIm	20
		2nd layer	AAm	40	DMAA	40	MAA	20

Table S2. Compositions of the various $A_mD_nX_o$ bilayered hydrogels keeping the AAm – DMAA ratio fixed at 5:3 following the results obtained from Table S1.

Entry	Sample	Composition (wt%)						
1	$A_{56.25}D_{33.75}X_{10}$	**1st layer**	AAm	56.25	DMAA	33.75	VIm	10
		2nd layer	AAm	56.25	DMAA	33.75	MAA	10
2	$A_{50}D_{30}X_{20}$	**1st layer**	AAm	50	DMAA	30	VIm	20
		2nd layer	AAm	50	DMAA	30	MAA	20
3	$A_{43.75}D_{26.25}X_{30}$	**1st layer**	AAm	43.75	DMAA	26.25	VIm	30
		2nd layer	AAm	43.75	DMAA	26.25	MAA	30
4	$A_{37.5}D_{22.5}X_{40}$	**1st layer**	AAm	37.5	DMAA	22.5	VIm	40
		2nd layer	AAm	37.5	DMAA	22.5	MAA	40

Table S3. Absorption peaks of the individual layers of the HA.

Entry	Constructs of HA	Absorption Peak (cm^{-1})	Functional Groups
1	VIm@AAm	3340	Stretching vibrations of NH_2
		3195	
		2917	C-H stretching vibrations of -CH and $-CH_2$ in the main polymeric chain
		1500	Stretching vibrations of N-C bonds in the imidazole ring
2	MAA@AAm	1655	C=O stretching vibration of the amide bond

Table S4. pH-dependent lifetime measurements of TPE4A and TPE4A@HA.

System	λ(nm)	pH	τ_1(ns)	τ_2(ns)	τ_{av}(ns)	χ^2
TPE4A	500	3	0.43	0.57	3.710	1
		11	0.02	0.98	0.013	0.98
TPE4A@HA	500	3	0.26	0.73	5.60	1
		11	0.37	0.63	3.40	1

Table S5. pH-dependent quantum yields of TPE4A@HA.

System	λ(nm)	pH	Φ%
TPE4A@HA	500	3	44.50
		11	1.61